RADIATION AND ABLATION COOLING FOR MANNED REENTRY VEHICLES

By Leonard Roberts

For Presentation at the Second International Congress of the Institute of the Aeronautical Sciences

Zurich, Switzerland
September 12-16, 1960

RADIATION AND ABLATION COOLING FOR MANNED REENTRY VEHICLES

By Leonard Roberts[1]

NASA Langley Research Center

SUMMARY

The necessity of reducing heat transfer to reentry vehicles has led to the consideration of both radiative and ablation shields. The paper reviews briefly the heating problems for manned vehicles and the means whereby ablation and radiation afford thermal protection.

The principal energy disposal and weight parameters are then presented and their relation to the vehicle and trajectory parameters is discussed. A comparative analysis of three types of ablation shield is made and broad conclusions are drawn as to the type of shield most appropriate to manned reentry vehicles.

SYMBOLS

$\frac{M}{C_D AR}$	$\frac{\text{Mass of vehicle}}{(\text{Drag coeff.})(\text{ref. area})(\text{nose radius})}$, slugs/cu ft
E	energy, ft-lb/slug
$\frac{E}{gJ}$	energy, Btu/lb
B	mass ratio parameter
L/D	lift-drag ratio
G	deceleration, g units

[1]Head, Mathematical Physics Branch.

q	heating rate, per unit area, Btu/sq ft/sec
Q	heat input, per unit area, Btu/sq ft
n	$\frac{1}{2}$ (laminar flow), $\frac{4}{5}$ (turbulent flow)
X	energy disposal parameter
ϵ	emissivity
σ	Stefan-Boltzmann constant
T	temperature ^{o}R
H	thermal capacity, Btu/lb
$\frac{c}{\rho k}$	$\frac{\text{Specific heat}}{(\text{Density})(\text{thermal conductivity})}$, $\frac{\text{secs}}{(\text{lb/sq ft})^2}$
W	weight per unit area, lb/sq ft
f	fraction of resin in composite shield
f'	fraction of resin vaporized
t	duration of heating, sec

Subscripts:

a	ablation
c	conduction, or circular
i	insulation, or initial
r	radiation
m	mean
b	back surface
g	gas produced by sublimation
l	liquid coolant
$*$	dimensionless quantity

INTRODUCTION

A vehicle entering the earth's atmosphere has excess potential and kinetic energy which must be disposed in a controlled manner if the vehicle is to survive. A large fraction of this energy is transferred to the atmosphere (as kinetic and heat energy), nevertheless the remainder, which appears as the aerodynamic heat input to the vehicle, is of such magnitude that its disposal constitutes a major problem.

The limited capacity of metals to absorb this heat has led to the use of two alternative methods of thermal protection. The first method is to radiate the heat from a high-temperature surface, the second is to supply material which is allowed to melt or vaporize, thereby absorbing heat.

Both methods involve additional weight. For the radiative system the weight is determined primarily by the emissivity of the surface, the thermal properties of the insulation necessary to maintain the high surface temperature, and the duration of the reentry; in the ablation system the weight is determined by the total aerodynamic heat input and by the total heat capacity of the ablation material. In assessing the merit of either approach we are mainly concerned with minimizing weight although in any practical application to manned vehicles, dependability and versatility are always important.

In this paper particular attention is given to the problem of thermal protection of vehicles which reenter the atmosphere from supercircular speeds (for example, a vehicle returning from a lunar flight). In order to better understand the nature of the heating environment to which such vehicles are exposed some discussion of their motion is required.

Here we are content to discuss in heuristic fashion the more important parameters which determine the aerodynamic effects of heating and deceleration. Consideration is then given to the manner in which radiation and ablation systems afford thermal protection with particular reference to the relationship between the thermal shield parameters and the vehicle design parameters.

MOTION AND HEATING OF MANNED REENTRY VEHICLES

The problem of reentry of manned vehicles into the earth's atmosphere has received much attention in recent years. Following the work of Allen and Eggers (ref. 1) on ballistic reentry, and Sanger (ref. 2) on the steady lifting glide, Chapman (refs. 3 and 4) has made a general study of the dynamics and heating experience of both lifting and nonlifting vehicles which reenter the atmosphere from circular or supercircular orbits. Further papers (refs. 5, 6, 7, and 8) on trajectory control through lift and drag modulation have added to our understanding of the subject.

In the present paper we will generally follow the work of Chapman although in order to obtain a qualitative understanding of the problem, a simple approximate solution is used. The energy equation for a vehicle of mass M, frontal area A, and drag coefficient C_D is written in terms of mass parameter B as follows:

$$E = E_i e^{-B(s)} \tag{1}$$

where E_i is the initial energy of the vehicle, $B = \dfrac{\int^s \rho C_D A \, ds}{M}$ and s is the distance travelled through the atmosphere.

If we consider the vehicle to travel down a tube of air of cross-sectional area C_DA (see fig. 1), then the mass of air in a length s of the tube is $\int^s \rho C_D A \, ds$, thus

$$B(s) = \frac{\text{Mass of air pushed aside by the vehicle}}{\text{Mass of the vehicle}}$$

and the energy of the vehicle is reduced by a factor e each time the vehicle pushes aside a mass of air equal to its own mass M. A vehicle which reenters at parabolic speed (35,000 ft/sec) must push aside a mass of air $7M$ in order to reduce its speed to sonic speed. This may be done either by using a tube of air of large cross section $\left(\text{corresponding to a vehicle of small } \frac{M}{C_DA}\right)$ or a tube of great length as obtained when a vehicle makes a shallow reentry with aerodynamic lift.

As shown by Chapman (ref. 4), there exists a narrow flight-path corridor through which reentry into the atmosphere must be made. The lower boundary of the corridor (termed the undershoot boundary) is determined by the condition that the vehicle shall not exceed a given maximum deceleration (say 10g). The upper boundary (the overshoot boundary) is determined by the condition that the vehicle, upon reentry, shall remain within the sensible atmosphere and complete the reentry maneuver in one pass.

If an exponential variation of atmospheric density with altitude is assumed, together with constant $\frac{M}{C_DA}$ and L/D, the vehicle deceleration at undershoot varies approximately as Be^{-B} and the maximum deceleration G_{max} occurs when $B = 1$, that is, when the vehicle has encountered a mass of air equal to its own mass M.

At overshoot, the vehicle must enter the atmosphere at a low enough altitude that it encounters sufficient air to reduce its energy from E_i to E_c. Thus, in the supercircular part of reentry ($E > E_c$) $B = \ln E_i/E_c$, that is, the mass of air encountered is $M \ln E_i/E_c$ and the vehicle is left in a near circular orbit at the edge of the earth's atmosphere, and in a position to complete reentry in one pass.

The width of the corridor depends on the initial energy of the vehicle and on its aerodynamic lift capability. The width may be increased by applying positive lift at undershoot and negative lift at overshoot; for a vehicle having parabolic energy (for example, a vehicle returning from a lunar flight) with $G_{max} = 10$ the width increases appreciably by using a moderate amount of lift (from 7 miles with $L/D = 0$ to 40 miles with $L/D = 1/2$ or 52 miles with $L/D = 1$). If the more severe limitation of $G_{max} = 5$ is imposed, the corridor width is correspondingly lower (the reader is referred to refs. 4 and 5 for a more complete discussion).

A vehicle returning through this corridor will experience a period of severe heating, the magnitude and duration of which depend on the vehicle characteristics and the type of trajectory it follows. For a trajectory near undershoot the heat-transfer rate q increases to a maximum value q_{max} (which occurs when the vehicle has traversed a mass of air $1/3\ M$ approximately for laminar flow or $8/15\ M$ for turbulent flow) and thereafter decreases. For a trajectory near overshoot, however, the heating rate has a maximum value $(q_{max})_1$ during the supercircular portion of the trajectory and decreases to a lower value at circular speed; thereafter it again increases to a second maximum value $(q_{max})_2$ during the descent from circular orbit and finally decreases to zero.

General, relatively simple, expressions for q_{max} and ΔQ at the nose of the vehicle for laminar flow or at the sonic point for turbulent flow are written as follows:

$$q_{max} = 590\left(\frac{M}{C_D A}\right)^n R^{n-1} q^* \quad \frac{Btu}{(sq\ ft)(sec)} \tag{2a}$$

$$\Delta Q = 15{,}900\left(\frac{M}{C_D A}\right)^n R^{n-1}\, \Delta Q^* \tag{2b}$$

where $n = 1/2$ for laminar flow and $n = 4/5$ for turbulent flow. For other regions the heating rates are generally lower and equations (2a) and (2b) must be used in conjunction with a multiplicative factor which depends on the vehicle geometry. The quantities q^* and ΔQ^* are functions of the initial energy, the L/D ratio and the type of trajectory; near undershoot, for example

$$q^* \propto (E_i/E_c)^{3/2-n}(G_{max})^n \quad \text{and} \quad \Delta Q^* \propto (E_i/E_c)^{2-n}(G_{max})^{n-1}$$

and it is seen that the maximum heating rate increases (whereas the total heat input decreases) as G_{max} increases. The dimensionless coefficients q^* and ΔQ^* are shown in table I for the undershoot and overshoot boundaries of a vehicle which reenters with parabolic energy ($E_i/E_c = 2$). At overshoot, the total heat input is the sum of the heat inputs during the supercircular and subcircular portions, $\Delta Q = \Delta Q_1 + \Delta Q_2$.

It is seen that q_{max} and ΔQ depend on a vehicle design parameter $\left(\frac{M}{C_D A}\right)^n R^{n-1}$, and on the trajectory through the coefficients q^* and ΔQ^*.

This dependence is shown more clearly in figure 2 for laminar flow. The undershoot and overshoot heating boundaries depend primarily on G_{max} and L/D, respectively; they appear as straight lines in a logarithmic plot of q_{max} against ΔQ and form a "heating corridor" in this plane.

As the boundaries of the reentry corridor are widened by employing lift (at overshoot), or by accepting a higher G_{max} (at undershoot), the heating corridor is also widened, making increased demands on the thermal protection system.

The location of the vehicle in this heating corridor depends on the aerodynamic parameters M/C_DAR and L/D (laminar flow). Here M/C_DAR is roughly interpreted as the density of the vehicle (for a solid sphere in hypersonic flow, with $C_D = 4/3$, $\frac{M}{C_DAR}$ is equal to the density in slugs/cu ft). The magnitude of both the heating rate and the total heat input increases as $\left(\frac{M}{C_DAR}\right)^{1/2}$ that is, as the square root of the vehicle density approximately. Here it is important that the interdependence of L/D and $C_D/C_{D_{max}}$ be recognized; since C_D decreases as L/D increases, the use of lift implies an increase in the total heat input to the vehicle.

The lines of constant $\frac{M}{C_DAR}$ are orthogonal to the boundary lines in figure 2. For each value of $\left(\frac{M}{C_{D_{max}}AR}\right)$ there is a rectangular region within the heating corridor which defines the range of possible values of q_{max} and ΔQ to which the vehicle may be subjected during reentry (the width of this rectangular region depends on the L/D - $C_D/C_{D_{max}}$ relationship, in fig. 2 the hypersonic drag polar with $(L/D)_{max} = 1$ was used).

Since corridor widening by the use of lift incurs a penalty in the form of increased heating, it is of interest to see the variation of

q_{max} and ΔQ with corridor width. This variation is shown in figures 3(a) and 3(b) for a vehicle having $\frac{M}{C_{D_{max}}AR} = 1$ entering with parabolic energy. From figure 3(a) it is seen that ΔQ increases rapidly at the overshoot boundary for $|L/D| > 1/2$ with little increase in corridor width. A similar increase in q_{max} at undershoot is noted for $L/D > 1/2$ (fig. 3(b)). It seems unlikely, therefore, that a lift/drag ratio of much more than 1/2 would be employed during the heating phase of reentry although greater amounts of lift may be desirable for the terminal phase.

Even with $|L/D| = 1/2$ the heating experience at undershoot and overshoot differ appreciably; ΔQ at overshoot is approximately three times that at undershoot, similarly q_{max} at undershoot is more than three times that at overshoot.

If the vehicle is to be allowed a wide flight-path corridor (40 miles with $|L/D| = 1/2$) the thermal protection system must be designed to withstand the high heating rates associated with undershoot reentry, and to dispose of the large total heat input associated with overshoot reentry.

Thus far we have considered only the convective heat input. However, because the gas layer between the vehicle and the shock radiates energy, there is an additional heat input to the vehicle, the magnitude of which depends primarily on E_i, $\frac{M}{C_D A}$, and R. Current preliminary estimates indicate that it is of the order of 10 to 25 percent of the convective heat input for presently conceived vehicles entering at parabolic speed (the latter amount at undershoot). The effect of this is to increase the magnitude (but not the duration) of the heat pulse. Quantitative results

for the gas-layer radiation heating are not presented herein although some qualitative discussion is given later.

THERMAL PROTECTION OF MANNED REENTRY VEHICLES

The problem of thermal protection is that of maintaining the structure of the vehicle below some required design temperature dictated by the structural materials used or by the contents within the vehicle. A good thermal shield may be defined as one which performs this function satisfactorily with a minimum of weight. In the present application to manned reentry vehicles we require the shield to operate efficiently for all trajectories between undershoot and overshoot in order to make maximum use of the reentry corridor.

Technology in the field of thermal protection has proceeded in two fairly independent directions during the last several years, due mainly to the dissimilar needs of the short-flight-duration ballistic missile and the long-flight-duration hypersonic airplane. These needs have been satisfied by the ablation shield and the high-temperature metallic radiation shield, respectively. In a sense, the manned reentry vehicle of low lift capability is a combination of hypersonic airplane and ballistic vehicle; its heating experience is qualitatively similar, at undershoot, to that of the ballistic vehicle and at overshoot to that of hypersonic airplane of longer flight duration. It is likely, therefore, that a combination radiation-ablation shield will be the most appropriate for the supercircular reentry vehicle.

Some analysis of metallic radiation shields applied to simple configurations has been made by Anderson and Brooks (ref. 9) but for heating

rates considerably less than those encountered during supercircular entry. Metallic radiation shields are temperature limited, can dispose of 30 to 40 Btu/(sq ft)(sec), and are generally inadequate for the heating rates encountered over the nose or leading surfaces during supercircular reentry. Radiating ablation materials, on the other hand, are not temperature limited and are therefore much more versatile.

In recent years much effort has been applied to the development and analysis of ablation materials, due largely to the requirements of the missile program. A large number of materials has been tested experimentally in a variety of high-temperature facilities (refs. 10 to 13); theoretically steady ablation (both melting and vaporization) has been treated extensively (refs. 14 to 20) and more recently some attempt has been made to account for the unsteady conduction effects within the ablation shield during reentry from a circular orbit (refs. 21 to 22).

In the present paper we consider the combined effects of ablation, radiation, and thermal conduction in conjunction with the vehicle and trajectory characteristics which determine them. Our purpose is to establish the principal parameters that determine shield weight requirements for a given vehicle. Although we cannot draw conclusions concerning the overall weight of a cooling system unless the complete configuration of the vehicle is considered, we can discuss regions of high heating on a separate basis. The reader is referred to a forthcoming NASA publication (ref. 23) for the expressions used in the analysis of weight requirements.

In theory, either the radiative or the ablation cooling approach can be applied to the manned reentry problem; in practice both systems are compromised to some extent by material limitations. The ablation materials

discussed herein have been placed in the following three broad categories according to the manner in which they dispose of heat energy:

(a) Low-temperature subliming materials

(b) Radiating high-temperature ablation materials

(c) Composite charring materials

A summary chart of typical materials is shown in figure 4. The low-temperature materials absorb heat in the phase charge and in the stream boundary layer (a description of this cooling mechanism may be found in ref. 17); Teflon and nylon are typical materials. The radiating ablation materials dispose of heat by radiation and ablation - opaque quartz and graphite are representative of this category. Finally, composite charring ablation materials are considered; here ablation takes place at a low temperature and causes a carbonaceous char to form. The char attains a high temperature, radiates energy at the surface, and also acts as insulation, thereby reducing heat conduction to the ablation surface (beneath the char layer). Phenolic nylon and phenolic glass are typical composite materials.

For a given heat input the total weight of the shield may be considered as the sum of two amounts: firstly, the weight actually lost by ablation (or charred by ablation) and secondly, the weight required to insulate against and absorb the heat that accumulates by conduction. The latter amount depends on the type of insulation-absorption system used between the shield and the vehicle structure.

One system is simply to add sufficient ablation material to ensure that the vehicle structure remains below its design temperature. that is, a "self-insulating shield." An alternative system is to add a layer of

ablation material to reduce conduction and a layer of liquid (between the ablation shield and the vehicle structure) which is allowed to vaporize and thereby absorb any accumulation of heat near the vehicle structure, that is, a "liquid-cooled shield." The energy disposal and weight parameters for such materials are discussed below.

ENERGY DISPOSAL PARAMETERS

In the most general case the aerodynamic heat input to the shield is balanced by ablation, radiation, and conduction of heat. If χ_a, χ_r, and χ_c are the respective fractional amounts of energy disposed by these three effects, then

$$\chi_a + \chi_r + \chi_c = 1$$

The expressions for χ_c for the self-insulating and liquid-cooled shield are written, respectively

$$\chi_c = \frac{2}{\sqrt{\pi}} \frac{\sqrt{2\left[c(T_m - T_b)\right]\left(\rho \frac{k}{c}\right)^{1/2}}}{(q_{max}\,\Delta Q)^{1/2}} \zeta_c, \quad \frac{\sqrt{2\left[c(T_m - T_b)H_c\right]^{1/2}\left(\rho \frac{k}{c}\right)^{1/2}}}{(q_{max}\,\Delta Q)^{1/2}} \zeta_c \tag{3}$$

where $\zeta_c \leq 1$ in each case.

The factor $(q_{max}\,\Delta Q)^{1/2}$ depends on the vehicle design parameters and the trajectory it follows during reentry. For laminar flow, however, $(q_{max}\,\Delta Q)^{1/2}$ is insensitive to the vehicle trajectory and may be written

$$(q_{max}\,\Delta Q)^{1/2} \approx 2\left(\frac{M}{C_D A R}\right)^{1/2}\left(\frac{E_i}{E_c}\right)^{5/4} \times 10^3 \tag{4}$$

For laminar flow, therefore

$$\chi_c \approx \sqrt{\frac{2}{\pi}} \times 10^{-3} \frac{c(T_m - T_b)\left(\rho \frac{k}{c}\right)^{1/2}}{\left(\frac{M}{C_D A R}\right)^{1/2}\left(\frac{E_i}{E_c}\right)^{5/4}}, \quad \frac{1}{\sqrt{2}} \times 10^{-3} \frac{\left[c(T_m - T_b)H_c\right]^{1/2}\left(\rho \frac{k}{c}\right)^{1/2}}{\left(\frac{M}{C_D A R}\right)^{1/2}\left(\frac{E_i}{E_c}\right)^{5/4}}$$

respectively. Thus,

$$\frac{\text{Heat accumulated by shield}}{\text{Aerodynamic heat input}} \propto \frac{\left(\text{Thermal capacity of shield}\right)}{(\text{Vehicle density})^{1/2}} \cdot \frac{\left(\text{Thermal resistance of shield}\right)^{-1/2}}{(\text{Vehicle energy})^{5/4}}$$

where $\left[c(T_m - T_b)H_c\right]^{1/2}$ is interpreted as the thermal capacity of the insulation layer plus liquid coolant and $\frac{c}{\rho k} \frac{\text{sec}}{(\text{lb/sq ft})^2}$ is the thermal resistance (that is, the number of seconds taken for heat to conduct through a layer of weight 1 lb/sq ft).

Estimation of the fraction of heat accumulated during reentry is now a simple matter. For a low-temperature material such as Teflon $\left(\frac{c}{\rho k} = 40 \frac{\text{sec}}{(\text{lb/sq ft})^2}, \; c(T_m - T_b) = 250 \text{ Btu/lb}\right)$ used on a vehicle of $\frac{M}{C_D A R} = 1$ entering with parabolic energy ($E_i/E_c = 2$) less than 1 percent of the aerodynamic heat input is accumulated. Even for a high-temperature material such as Foamed Quartz $\left(\frac{c}{\rho k} = 60 \frac{\text{sec}}{(\text{lb/sq ft})^2}, \; c(T_m - T_b) = 1{,}000 \text{ Btu/lb}\right)$ less than 3 percent is accumulated. It is interesting to note that for graphite, however $\left(\frac{c}{\rho k} = 1 \frac{\text{sec}}{(\text{lb/sq ft})^2}, \; c(T_m - T_b) = 2{,}000 \text{ Btu/lb}\right)$ as much as 40 percent is accumulated in the same circumstances. Obviously, $\frac{c}{\rho k}$ should be as large as possible so that accumulation of heat is minimized. In the discussion that follows it is assumed that $\chi_c \ll 1$.

The quantities χ_a, χ_r, and T_m depend on the ablation temperature T_a and the heating rate $q_{max} = \sigma\epsilon T_{max}^4$ (where T_{max} is a reference temperature associated with radiative equilibrium at $q = q_{max}$) and are written, for $\frac{T_a}{T_{max}} \leq 1$

$$\chi_a = 1 - \chi_r = 1 - 2\left(\frac{T_m}{T_{max}}\right)^4 = \left[1 - \left(\frac{T_a}{T_{max}}\right)^4\right]^2 \qquad (5)$$

When aerodynamic heating and radiative cooling produce thermal equilibrium $\left(\text{no ablation, } \frac{T_a}{T_{max}} \geq 1\right)$ then $\chi_a = 0$, $\chi_r = 1$, and $\frac{T_m}{T_{max}} = (1/2)^{1/4}$. From figure 5 and the definition of χ_c we see that there is an important dependence of χ_c on χ_a through the mean temperature T_m.

The energy $\chi_a \Delta Q$ which must be disposed by ablation may be reduced by using a high-temperature ablation material $\left(\frac{T_a}{T_{max}} \to 1\right)$ but only at the expense of increasing the accumulated energy $\chi_c \Delta Q$ $\left(\text{since } \frac{T_m}{T_{max}} \to (1/2)^{1/4}\right)$. Furthermore, it is seen that little is to be gained by using moderately high-temperature ablation materials; when $\frac{T_a}{T_{max}} = 1/2$, for example, χ_a differs little from unity but $\frac{T_m}{T_{max}}$ has increased from 0 to 1/2, with a corresponding increase in $\chi_c \Delta Q$.

Since q_{max} varies appreciably between undershoot and overshoot, the behavior of the radiating ablation shield also varies. For example, if $\frac{M}{C_{D_{max}} AR} = 1$ and $L/D = 1/2$, then $q_{max} = 550$ Btu/(sq ft)(sec) at undershoot, and a shield with $T_a = 4{,}000^\circ$ R, $\epsilon = 1/2$, would have $\chi_a = 0.8$ approximately indicating that 80 percent of the aerodynamic heat input is disposed by ablation and approximately 20 percent by radiation. At overshoot, on the other hand, $(q_{max})_1 = 150$ Btu/(sq ft)(sec) for the supercircular part of reentry and only 33 percent is disposed by ablation,

whereas for the descent from circular orbit $(q_{max})_2 = 75$ Btu/(sq ft)(sec), less than 3 percent is disposed by ablation and the shield is in near radiative equilibrium.

MEAN EFFECTIVE HEAT CAPACITY

For subliming materials, the effective heat capacity has been shown theoretically to be an approximately linear function of the stream energy and is written

$$H_{eff} = H_a + \beta_a \frac{E}{gJ} \tag{6a}$$

Here H_a is the energy absorbed when unit mass of material is raised to the ablation temperature and undergoes vaporization, β_a is the fraction of the stream energy absorbed by the gas products during convection in the boundary layer, and $\frac{E}{gJ}$ is the energy of the stream in thermal units. Typical values of materials presently being considered are $H_a = 1{,}000$ Btu/lb, $\beta_a = 1/2$ (laminar flow) or $\beta_a = 1/4$ (turbulent flow). The turbulent values of β_a are generally about one-half or one-third of the laminar values. When $\beta_a = 1/2$, for example, the material in gaseous form absorbs an amount of the order of one-half of the stream energy $\left(\frac{E}{gJ} = 13{,}500 \text{ Btu/lb at circular energy}\right)$ in addition to the heat of sublimation H_a. The form of H_{eff} suggests that a mean value for the complete reentry should be written

$$H_m = H_a + \beta_a \frac{\mu E_i}{gJ} \tag{6b}$$

where μE_i is a mean value of E. For a vehicle reentering in a steady glide, for example, H_m may be evaluated analytically and is written, in dimensionless form

$$\frac{H_m}{H_a} = (1 - n)\left[1 + \left(1 + \frac{\beta_a \frac{E_i}{gJ}}{H_a}\right)^{-(1-n)}\right]^{-1} \frac{\beta_a \frac{E_i}{gJ}}{H_a}$$

and it may be verified that

$$1 + (1 - n)\frac{\beta_a \frac{E_i}{gJ}}{H_a} \leq \frac{H_m}{H_a} < 1 + \left(1 - \frac{n}{2}\right)\frac{\beta_a \frac{E_i}{gJ}}{H_a}$$

$\left(\text{that is, } 1 - n < \mu < 1 - \frac{n}{2}\right)$ where $n = 1/2$ (laminar flow) or $n = 4/5$ (turbulent flow). A dimensionless plot of $\frac{H_m}{H_a}$ versus $\frac{\beta_a \frac{E_i}{gJ}}{H_a}$ is shown in figure 6; also shown are values calculated numerically for return along the undershoot boundary for a nonlifting vehicle. Although the trajectory differs considerably from the equilibrium glide, the values of $\frac{H_m}{H_a}$ are in good agreement. For entry along the overshoot boundary, the supercircular and subcircular parts are treated separately. Here we use

$$(H_m)_1 = H_a + \frac{\beta_a E_c}{gJ} + \frac{\beta_a \mu (E_i - E_c)}{gJ} \quad \text{(supercircular)}$$

$$(H_m)_2 = H_a + \beta_a \frac{\mu E_c}{gJ} \quad \text{(subcircular)}$$

It is noted that the turbulent value of $\beta_a \mu$ may be as little as 1/5 of the laminar value and sublimation is much less efficient when turbulent flow prevails.

WEIGHT PARAMETERS

The weight of the ablation shield depends on the efficiency with which the amounts of heat $\chi_c \Delta Q$ and $\chi_a \Delta Q$ are disposed. Considering first the accumulated heat $\chi_c \Delta Q$, the associated weight W_c is written approximately $W_c = \dfrac{\chi_c \Delta Q}{c(T_b - T_{b,i})}, \dfrac{\chi_c \Delta Q}{\frac{1}{2} H_c}$, respectively, for the self-insulated shield and the liquid-cooled shield. When the appropriate expressions for χ_c (eq. (3)) are inserted, we obtain the following result:

$$(W_c)_{\text{self-insulated}} > (W_c)_{\text{liquid cooled}} \quad \text{if} \quad \frac{\left[c(T_m - T_b)H_c\right]^{1/2}}{c(T_b - T_{b,i})} > \sqrt{\pi} \tag{7}$$

approximately. The inequality (7) is a particularly simple condition inasmuch as it involves only the "thermal capacities" $\left[c(T_m - T_b) \cdot H_c\right]^{1/2}$ and $c(T_b - T_{b,i})$.

If the ablation temperature is sufficiently low, the self-insulated shield weighs less than the liquid-cooled shield. For a radiating ablation shield, however, where $T_m - T_b$ is necessarily large, the liquid-cooled system is more appropriate. For example, if we suppose that $c = 0.3$ Btu/lb $^{\circ}$R and $H_c = 1{,}000$ Btu/lb (corresponding to the vaporization of water) then equation (7) shows that the water-cooled system weighs less when $T_m - T_b > 230^{\circ}$ R.

It is clear, therefore, that the water-cooled system is preferred unless the vehicle structure is designed to withstand temperatures fairly close to the mean surface temperature of the shield.

As we noted earlier, the accumulated heat $\chi_c \Delta Q$ depends on χ_a through the mean temperature T_m; it is to be expected therefore that W_c depends on W_a. This dependence is illustrated more clearly when we consider the liquid-cooled shield in more detail. We denote by W_a, W_i, and W_l the weight of material lost by ablation, the additional weight required for insulation, and the weight of liquid required to absorb the accumulated energy. The total weight W is written $W = W_a + W_i + W_l$ (so that $W_c = W_i + W_l$). The actual weight loss caused by ablation is simply $W_a = \frac{\chi_a \Delta Q}{H_m}$ $\left(\text{or } \left(\frac{\chi_a \Delta Q}{H_m}\right)_1 + \left(\frac{\chi_a \Delta Q}{H_m}\right)_2 \text{ at overshoot}\right)$. The expressions for W_c and χ_c suggest that we define a dimensionless weight parameter W^* through

$$W^* = W\left\{\left(\frac{\rho k}{c}\right)\frac{\left[c(T_m - T_b)\,\frac{\Delta Q}{q_{max}}\right]_1 + \left[c(T_m - T_b)\,\frac{\Delta Q}{q_{max}}\right]_2}{\frac{1}{2} H_c}\right\}^{-1/2} \tag{8}$$

The weights W_i and W_l are chosen so that W is a minimum. This gives the following expressions for W_i^* and W_l^* in terms of $W_a^* = W_{a,1}^* + W_{a,2}^*$

$$W_i^* = \frac{1}{2} W_a^* \left[\sqrt{1 + \left(\frac{1}{2} W_a^*\right)^{-2}} - 1\right] \tag{9}$$

and

$$W_l^* = \frac{1}{W_a^*} \log_e\left(1 + \frac{W_a^*}{W_i^*}\right) \tag{10}$$

(at undershoot $\Delta Q = (\Delta Q)_1$ and $\Delta Q_2 = 0$).

Figure 7 shows $W_a^* + W_i^*$ and W_l^* as functions of W_a^*. The two limiting cases $W^* \to \infty$ and $W^* \to 0$ are interesting since they give us the important ablation and radiation weight parameters.

Firstly, as $T_m - T_b \to 0$, $\chi_a \to 1$ and equation (8) shows that $W^* \to \infty$; thus for the low-temperature ablation shield W_i and W_l are small compared with W_a (in practice when $W_a^* > 10$) and we may write

$$W = W_a = \left(\frac{\Delta Q}{H_m}\right)_1 + \left(\frac{\Delta Q}{H_m}\right)_2 \qquad (11)$$

and for a given heat input W may be reduced only by increasing H_m.

Secondly, when $\chi_a = 0$, $W_a^* = 0$, no ablation takes place and the shield acts as a radiation shield. (It should be noted, however, that $\chi_a = 0$ only if $\frac{T_a}{T_{max}} \geq 1$, that is, if the ablation temperature T_a exceeds $\left(\frac{q_{max}}{\sigma\epsilon}\right)^{1/4}$). When $W_a^* = 0$, then $W_i^* = W_l^* = 1$ indicating that the shield should comprise equal weights of insulation and liquid coolant. Thus

$$W = W_i + W_l = 2\left\{\left(\frac{\rho k}{c}\right)\frac{\left[c(T_m - T_b)\frac{\Delta Q}{q_{max}}\right]_1 + \left[c(T_m - T_b)\frac{\Delta Q}{q_{max}}\right]_2}{\frac{1}{2}H_c}\right\}^{1/2} \qquad (12)$$

and since $T_{m,1}$ and $T_{m,2}$ are necessarily high in practical applications the weight may be reduced by increasing the thermal resistance $\frac{c}{\rho k}$ or the thermal capacity of the coolant H_c.

It is useful to have some criterion to indicate which type of shield is most suitable for a given vehicle; from equations (11) and (12) at undershoot we see that the radiating ablation shield weighs less than the low-temperature shield if

$$\left(\frac{M}{C_D A R}\right)^{1/2}\left(\frac{E_i}{E_c}\right)^{1/4} \cdot \frac{\left(\frac{c}{\rho k}\right)^{1/2}\left[\frac{\frac{1}{2}H_c}{c(T_m - T_b)}\right]^{1/2}}{\left(1 - \frac{2}{3}n\right)\beta_a\left(\frac{E_c}{gJ} \times 10^{-3}\right)} > 1 \qquad (13)$$

(to obtain eq. (13), the effective heat capacity is approximated by $H_m \approx \left(1 - \frac{2}{3} n\right) \beta_a \frac{E_i}{E_c} \frac{E_c}{gJ}$ and eq. (4) is used).

Inspection of the individual factors in equation (13) shows that the radiating ablation approach is more appropriate for the heavier vehicles providing $\frac{c}{\rho k}$, the thermal resistance, is large enough. This is especially true if considerable turbulent flow is experienced. $\left(\beta_a\left(1 - \frac{2}{3} n\right)\right.$ is smaller for turbulent flow than for laminar flow.$\left.\right)$ Equation (13) also applies at overshoot if used with an appropriate mean value T_m.

COMPARISON OF TYPICAL MATERIALS

The difference between the low-temperature subliming materials and the radiating ablation materials is illustrated by comparing the behavior of Teflon with that of Foamed Quartz (both water-cooled) at the stagnation point of a vehicle with $\frac{M}{C_{D_{max}} AR} = 1$ entering with parabolic energy, $\frac{E_i}{E_c} = 2$. The weight required per unit area (including that of the water) is shown in figures 8(a) and 8(b) for these materials.

Firstly, we see that the weight at overshoot always exceeds that at undershoot; thus, the weight requirements are dictated by overshoot conditions. Secondly, the weight at overshoot increases rapidly with L/D for $|L/D| > 1/2$; thus, extension of the corridor at overshoot is costly, whereas at undershoot the use of lift up to about $L/D = 1$ seems justified since the associated weight is still less than that at overshoot with $L/D = -1/2$. Thirdly, the radiating Foamed Quartz shield weighs less than the Teflon shield, especially at overshoot where a considerable

fraction of the energy is radiated (at undershoot, both materials act primarily as simple ablators and there is little difference in weight).

As we might expect, the behavior of the materials differs considerably at overshoot. For L/D = -1/2, the low-temperature Teflon suffers considerable weight loss - 20 lb/sq ft or about 2 inches in thickness - but requires only a small amount of water, 2.4 lb/sq ft, to absorb the accumulated heat. The radiating Foamed Quartz, however, loses only 2.3 lb/sq ft or about 0.3 inch, whereas the insulation plus coolant weight is 11 lb/sq ft. (By comparison, a water-cooled graphite shield would weigh in the neighborhood of 110 lb/sq ft, approximately half of which would be water.)

Quite generally the low-temperature subliming materials are subject to large weight loss and possible large changes in shape, whereas the radiating materials require a substantial amount of liquid coolant between the shield and the vehicle structure. In any practical application the weight of the coolant container and any piping required to remove the vapor must also be considered.

The third type of ablation shield, the composite shield, is a compromise between the low-temperature and the radiating materials. It consists of a high-temperature matrix impregnated with a low-temperature ablation material. In the fiberglass and phenolic shield, for example, ablation of the phenolic resin takes place at about 1,500° R and forms a high-temperature char layer held by the fiberglass matrix. A large fraction of the heat input is disposed by radiation at the surface of the char and the small fraction of heat that reaches the virgin material (by conduction through the char) is absorbed by the phase change in the

resin at a low temperature. The gas produced by this ablation diffuses through the char to the surface and helps to reduce conduction. (See fig. 8(c).)

The composite material, therefore, takes advantage of surface radiation (surface temperatures over $5,000^{\circ}$ R and an emissivity of 0.8 gives a rate of heat disposal of over 250 Btu/sq ft/sec) but at the same time retains the advantage of requiring little or no liquid coolant – ablation of low-temperature resin replaces vaporization of water as the back-surface-temperature control, essentially.

Conservative values (upper limits) of the mean surface temperature T_m and the char weight W are given by

$$\frac{T_m}{T_{max}} = \left(\frac{1}{2}\right)^{1/4} \tag{14a}$$

and

$$W = 2\left(\frac{\rho k_{char}}{c_g}\right)^{1/2}\left\{\left[\frac{c_g(T_m - T_a)}{f\left(H_a + f' c_g(T_m - T_a)\right)}\frac{\Delta Q}{q_{max}}\right]_1 + \left[\frac{c_g(T_m - T_a)}{f\left(H_a + f' c_g(T_m - T_a)\right)}\frac{\Delta Q}{q_{max}}\right]_2\right\}^{1/2} \tag{14b}$$

It is seen that equation (14b) is analogous to equation (12) with H_c replaced by $2f\left(H_a + f' c_g(T_m - T_a)\right)$ so that the cooling capacity of the resin increases with the surface temperature T_m. The importance of this is seen when the limit of large T_m is taken in equation (14b); the char weight has an upper limit

$$W < \sqrt{2}\left(\frac{\rho k_{char}}{c_g}\right)^{1/2}\left(\frac{t}{ff'}\right)^{1/2}$$

independent of the heating history, where $t = \left(\frac{\Delta Q}{\frac{1}{2} q_{max}}\right)_1 + \left(\frac{\Delta Q}{\frac{1}{2} q_{max}}\right)_2$ is a measure of the duration of heating. The accumulation in the virgin material is similar to that in a low-temperature ablation material and by choosing a resin which sublimes at a low temperature the shield can be self-insulated (the corresponding weight W_c is determined as before but with T_m replaced by T_a). The importance of high thermal resistance of the char and large heat of sublimation of the resin, H_a, is evident from equation (14b). Although current charring materials have lower thermal resistance than Foamed Quartz, their surface temperature and emissivity are higher and, for this reason, they have greater potential to dispose of high heat-transfer rates. Figure 8(c) shows typical values of the weight, including self-insulation for a range of corridor width (or L/D) for $\frac{M}{C_{D_{max}} AR} = 1$, with $T_a = 1{,}250^\circ$ R, $T_b - T_{b,i} = 500^\circ$ R, $f' = 0.4$, $f'' = 0.5$, $H_a = 1{,}250$ Btu/lb, and $\frac{c_g}{\rho k_{char}} = 40 \frac{\text{sec}}{(\text{lb/sq ft})^2}$.

DISCUSSION

The results presented thus far have been for $\frac{M}{C_{D_{max}} AR} = 1$. The variation of weight with $\left(\frac{M}{C_{D_{max}} AR}\right)^{1/2}$ is shown for overshoot reentry with $|L/D| = 1/2$ for three representative materials in figure 9. The character of the three curves is important. The low-temperature material has an essentially linear variation of weight with $\left(\frac{M}{C_{D_{max}} AR}\right)^{1/2}$ (indicating that the weight is proportional to the heat input); the weight of the foamed radiating material is nonlinear initially ($W \approx W_c$ varies

as $(T_m - T_b)^{1/2} \sim q_{max}^{1/8}$) but then becomes approximately linear for higher values of $\left(\frac{M}{C_{D_{max}}AR}\right)$ when appreciable ablation takes place. The curve for the composite material lies above the foamed material initially (it has lower thermal resistance $\frac{c}{\rho k}$), but for the higher values of $\frac{M}{C_{D_{max}}AR}$ it falls below the foamed material (since it continues to radiate at a higher surface temperature).

For each class of material there is a range of $\frac{M}{C_{D_{max}}AR}$ in which a shield of that material weighs less than the others. The location of the crossover points in figure 9 depends on the material properties, of course, so they are not well defined. When plots similar to figure 9 are made for other values of L/D a more general chart is obtained showing the relation between the vehicle parameters, $\frac{M}{C_{D_{max}}AR}$ and L/D, and the characteristics of the shield. This chart is shown in figure 10; we see that the three classes of material (a), (b), and (c) are appropriate to vehicles of small, intermediate, and large $\frac{M}{C_{D_{max}}AR}$, respectively, that is, to vehicles which experience small, intermediate, and large heating rates per unit area, respectively. The tendency for vehicles of higher lift-drag ratio to require a composite ablation material results from the lower values of $\frac{C_D}{C_{D_{max}}}$, and therefore higher heating rates, associated with higher values of L/D.

The conclusions drawn from figure 10 are based on the assumption of laminar convective heating; the possibility of turbulent heating and additional heating from the radiating gas layer must be recognized, however. It may be recalled that the mean effective heat capacity in turbulent flow is less than that for laminar flow, moreover in the

presence of gas layer radiation the linear increase of effective heat capacity with stream enthalpy no longer holds, the effective heat capacity is reduced and the actual weight loss may increase considerably.

This effect is most evident for the low-temperature materials and, to a lesser extent, for the foamed radiating materials if they undergo considerable ablation as at undershoot. The charring composite materials are least affected by these increases in heating since ablation of the resin depends primarily on conduction through the char rather than on the form of the heat input to the surface (the result is simply an increase in surface temperature and a minor increase in weight).

The final choice of materials will depend on mechanical as well as thermal properties. The foamed materials and the charring materials must have sufficient strength to withstand vibration and shear forces and long-duration tests of these materials are therefore desirable before they can be used with confidence. In view of the potential versatility of ablation materials for manned-flight application, considerable effort is warranted in the development of materials having the appropriate thermal and mechanical behavior.

It seems unlikely that the low-temperature materials will be used over the nose or leading surfaces where high heating rates are experienced and where gas layer radiation is greatest; however, they may be used in limited amounts for other parts of the vehicle which experience lower heating rates. The foamed materials weigh a little less than the self-insulated composite materials for intermediate heating levels but they cannot be used without a reservoir of liquid coolant between the shield and the vehicle.

The simplicity of the composite shield and its relative insensitivity to the form of heat input make it particularly attractive as a means of thermal protection for manned reentry vehicles.

CONCLUDING REMARKS

Supercircular entry into the earth's atmosphere can be made only through a narrow reentry corridor. The high rates of heat transfer associated with entry along the undershoot boundary of the corridor and the high total heat input experienced during entry along the overshoot boundary demand a versatile form of thermal protection.

A review of the types of ablation material aviilable shows that

(a) The low-temperature ablators may lose a considerable amount of material especially at overshoot; moreover turbulent heating and gas-layer radiation can increase the weight loss appreciably.

(b) Foamed radiating materials are less affected by the form of heat input (that is, whether laminar or turbulent convective, or radiative) and there is little actual weight loss. However, these materials require a reservoir of vaporizing liquid coolant between the shield and the vehicle structure to absorb the conducted heat.

(c) The composite charring materials generally have a lower thermal resistance than the foamed materials but because ablation takes place at a low temperature within the char layer they are self-insulating and may be used without additional liquid coolant. The composite materials are least affected by the form of heat input.

For manned reentry from supercircular speeds it appears therefore that the radiating ablation materials are more appropriate than the

low-temperature materials. In particular, the simplicity of the self-insulating composite shield and its ability to protect against radiative as well as convective heating make it an attractive solution to the problem of thermal protection.

REFERENCES

1. Allen, H. Julian, and Eggers, A. J., Jr.: A Study of the Motion and Aerodynamic Heating of Missiles Entering the Earth's Atmosphere at High Supersonic Speeds. NACA TN 4047, 1957.
2. Sanger, Eugen: Raketen-Flugtechnik. R. Oldenbourg (Berlin), 1933.
3. Chapman, Dean R.: An Approximate Analytical Method for Studying Entry Into Planetary Atmospheres. NACA TN 4276, 1958.
4. Chapman, Dean R.: An Analysis of the Corridor and Guidance Requirements for Supercircular Entry Into Planetary Atmospheres. NASA TR R-55,
5. Phillips, Richard L., and Cohen, Clarence B.: Use of Drag Modulation to Reduce Deceleration Loads During Atmospheric Entry. American Rocket Society Journal, vol. 29, no. 6, June 1959, pp. 414-422.
6. Lees, Lester, Hartwig, Frederic W., and Cohen, Clarence B.: The Use of Aerodynamic Lift During Entry Into the Earth's Atmosphere. American Rocket Society Journal, vol. 29, no. 9, September 1959, pp. 633-641.
7. Grant, Frederick C.: Importance of the Variation of Drag With Lift in Minimization of Satellite Entry Acceleration. NASA TN D-120, 1959.
8. Grant, Frederick C.: Analysis of Low Acceleration Lifting Entry From Escape Speed. NASA TN D-249.
9. Anderson, Roger A., Brooks, William A., Jr.: Effectiveness of Radiation as a Structural Cooling Technique for Hypersonic Vehicles. Journal of Aeronautical Sciences, vol. 27, no. 1, January 1960.

10. Chicago Midway Laboratories: Determination of Factors Governing Selection and Application of Materials for Ablation Cooling of Hypervelocity Vehicles, Qtrly. Progress Rep., June-September 1958, CML-TN-M131-11.

11. Grunfest, I. J., and Shenker, L. H.: Behavior of Reinforced Plastics at Very High Temperatures. Modern Plastics, June 1958.

12. Steg, L.: Materials for Re-Entry Heat Protection of Satellites. Presented at ARS Semi-Annual Meeting, San Diego, June 1959.

13. Brogan, T.: Electric Arc Gas Heaters For Re-Entry Simulation and Space Propulsion. Presented at the ARS 13th Annual Meeting, November 17-21, 1958, ARS preprint no. 724-58.

14. Sutton, G. W.: The Hydrodynamics and Heat Conduction of a Melting Surface. Jour. Aero/Space Sci., vol. 28, no. 1, 1958, p. 29.

15. Roberts, L.: On the Melting of a Semi-Infinite Body of Ice Placed in a Hot Stream of Air. Jour. Fluid Mech., vol. 4, part 5, September 1958, pp. 505-528.

16. Lees, L.: Similarity Parameters for Surface Melting of a Blunt Nosed Body in a High Velocity Gas Stream. American Rocket Society Journal, vol. 29, no. 5, May 1959, pp. 345-354.

17. Roberts, Leonard: A Theoretical Study of Stagnation-Point Ablation. NASA TR R-9, 1959.

18. Bethe, H. A., and Adams, Mac C.: A Theory for the Ablation of Glassy Materials. Jour. Aero/Space Sci., vol. 26, no. 6, June 1959, pp. 321-328.

19. Lew, H. G., and Fanucci, J. B.: A Study of Melting Surfaces. Aerophysics Research Memo 38, General Electric Rep. R59SD381, April 1959.

20. Gross, J. J., Masson, D. J., and Gazley, C., Jr.: General Characteristics of Binary Boundary Layers With Applications to Sublimation Cooling. Rand Rep. P-1371, May 8, 1958.

21. Adams, Mac C.: Recent Advances in Ablation. American Rocket Society Journal, vol. 29, no. 5, May 1959, pp. 625-632.

22. Roberts, Leonard: An Analysis of Ablation-Shield Requirements for Manned Reentry Vehicles. NASA TR R-62, 1960.

23. Roberts, Leonard: Prospective NASA Technical Note.

TABLE I.- DIMENSIONLESS HEAT-TRANSFER COEFFICIENTS

(a) Overshoot, laminar flow

$E > E_c$				$E < E_c$		
$\lvert L/D \rvert$	q_1^*	ΔQ_1^*	G_{max_1}	q_2^*	ΔQ_2^*	G_{max_2}
0	0.31	2.4	3.3	0.21	1.1	8.3
1/4	.26	3.1	2.0	.15	1.7	4.1
1/2	.22	3.7	1.4	.105	3.0	2.25
1	.19	4.6	1.05	.075	4.3	1.40

(b) Undershoot

$G_{max} = 10$					$G_{max} = 5$			
$\lvert L/D \rvert$	Laminar		Turbulent		Laminar		Turbulent	
	q^*	ΔQ^*	q^*	ΔQ^*	q^*	ΔQ^*	q^*	ΔQ^*
0	0.725	2.1	0.41	1.36	0.51	3.0	0.24	1.57
1/4	.76	2.1	.40	1.37	.54	3.0	.23	1.58
1/2	.77	2.22	.37	1.39	.54	3.15	.22	1.60
1	.77	2.5	.31	1.46	.54	3.5	.18	1.68

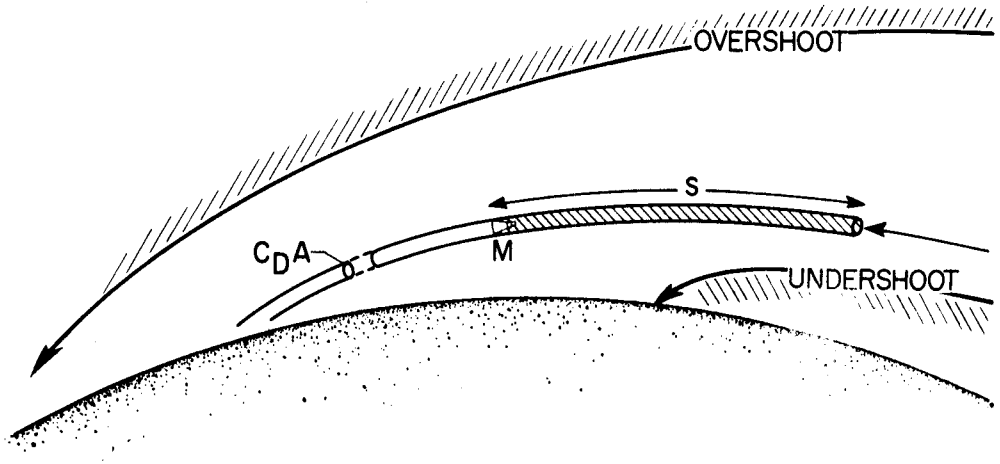

ENERGY: $E = E_i \exp\left(-\frac{M_{air(s)}}{M}\right)$

FLIGHT CONDITION (UNDERSHOOT ENTRY)	MASS OF AIR ENCOUNTERED
PEAK HEATING (LAMINAR)	$\frac{1}{3}M$
PEAK HEATING (TURBULENT)	$\frac{8}{15}M$
PEAK DECELERATION	M
CIRCULAR SPEED	(log 2) M
SONIC SPEED	7 M (PARABOLIC ENTRY)

NASA

Figure 1.- Motion and heating history.

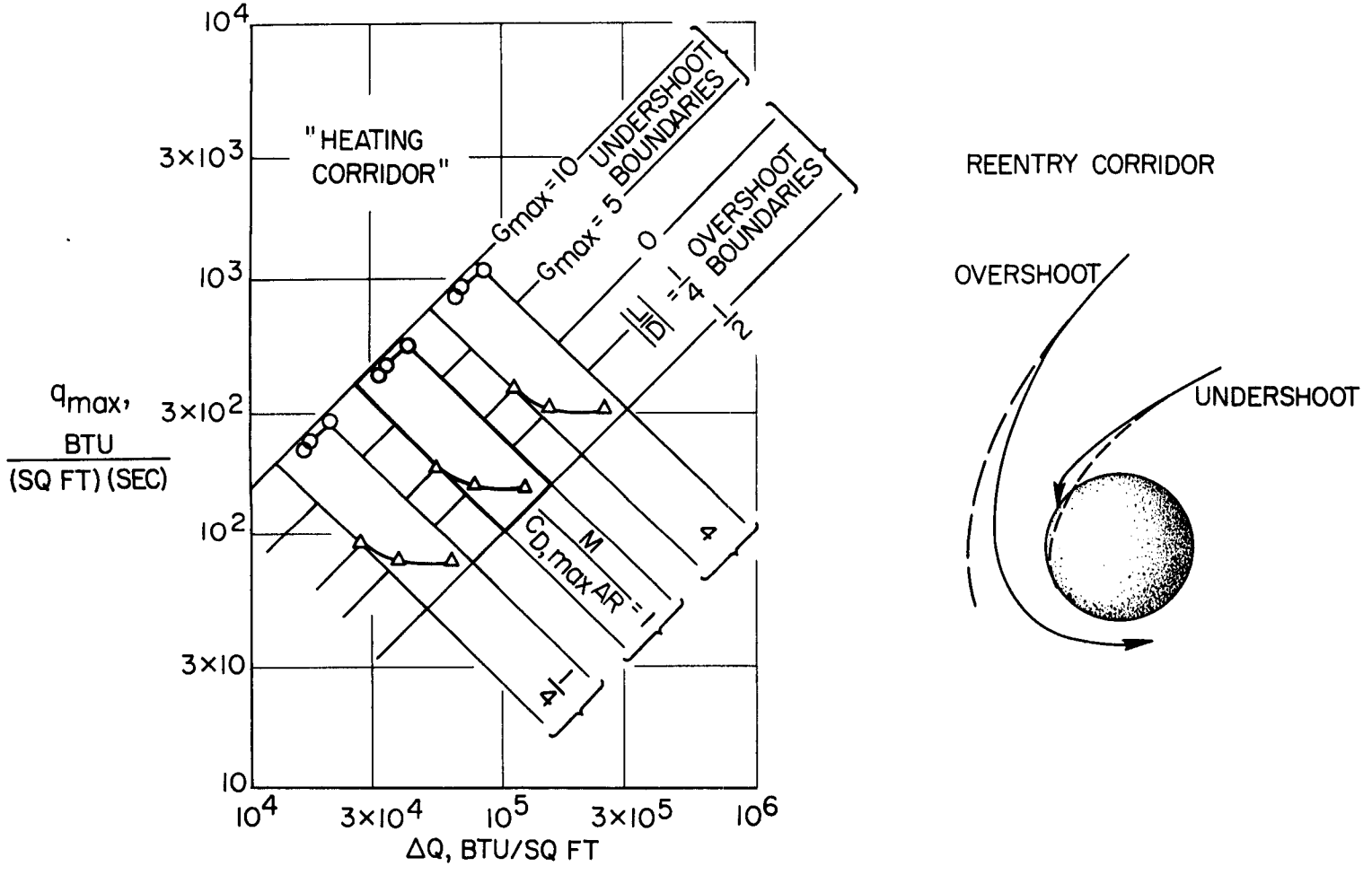

Figure 2.- Thermal environment-vehicles entering with parabolic energy, $\frac{E_i}{E_c} = 2$.

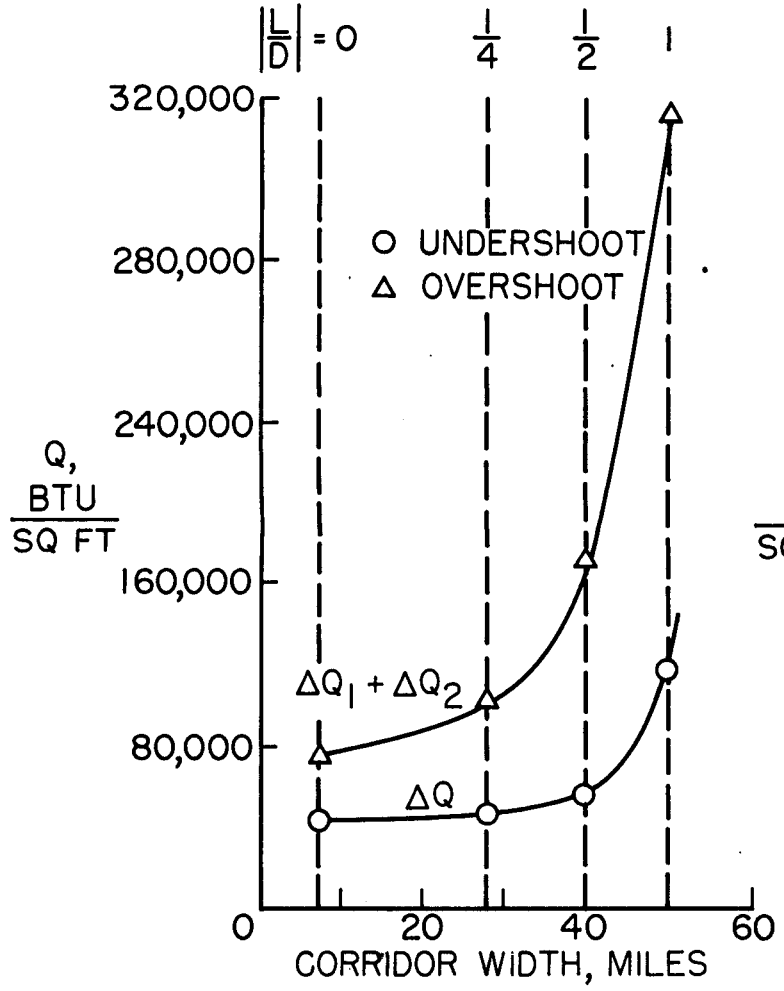

(a) Total heat input per unit area.

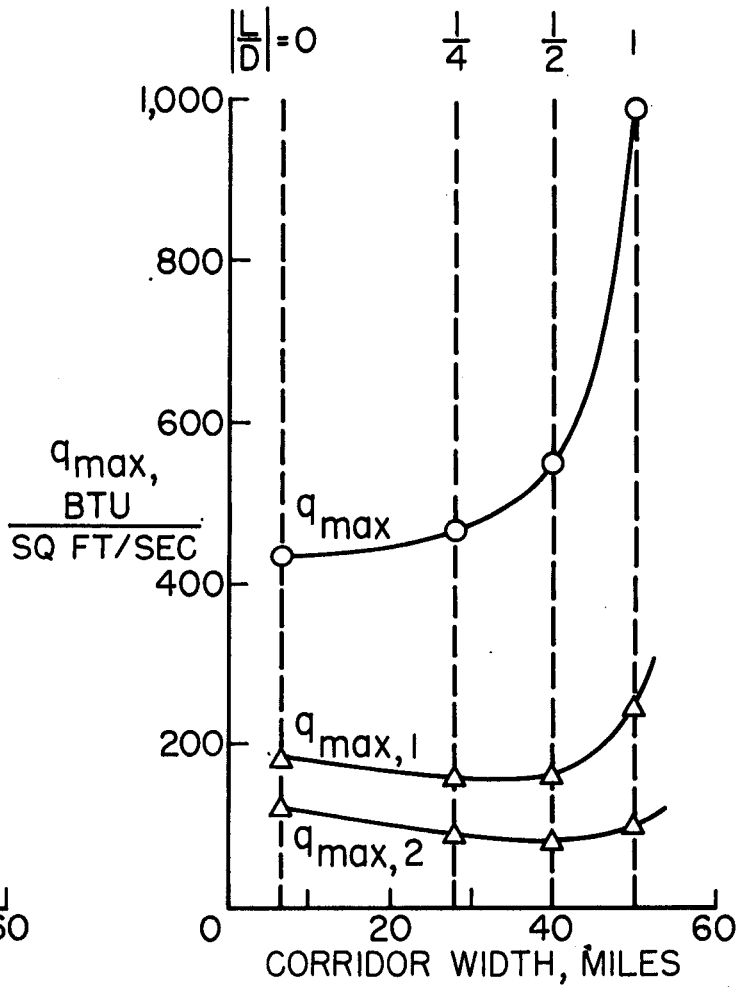

NASA

(b) Maximum convective heating rate per unit area.

Figure 3.- Variation of thermal environment with corridor width $\left[\left(\frac{E_i}{E_c}\right) = 2, \frac{M}{C_{D_{max}} AR} = 1\right]$

CLASS	ENERGY DISPOSAL	TYPICAL MATERIALS	BEHAVIOR
LOW-TEMPERATURE ABLATORS	PHASE CHANGE; BOUNDARY LAYER	TEFLON; NYLON	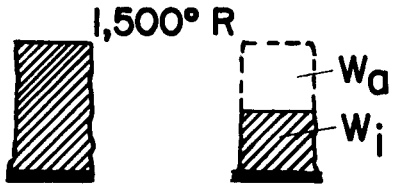
HIGH-TEMPERATURE ABLATORS	RADIATION; PHASE CHANGE	FOAMED QUARTZ; FIBER GLASS	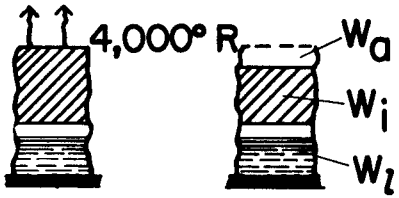
COMPOSITE CHARRING ABLATORS	RADIATION; PHASE CHANGE	FIBER GLASS AND PHENOLIC; NYLON AND PHENOLIC	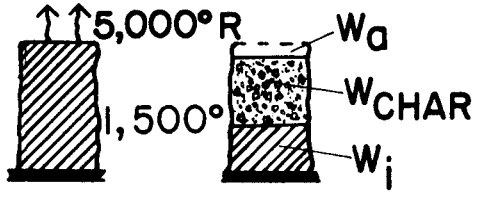

NASA

Figure 4.- Classification of ablation materials.

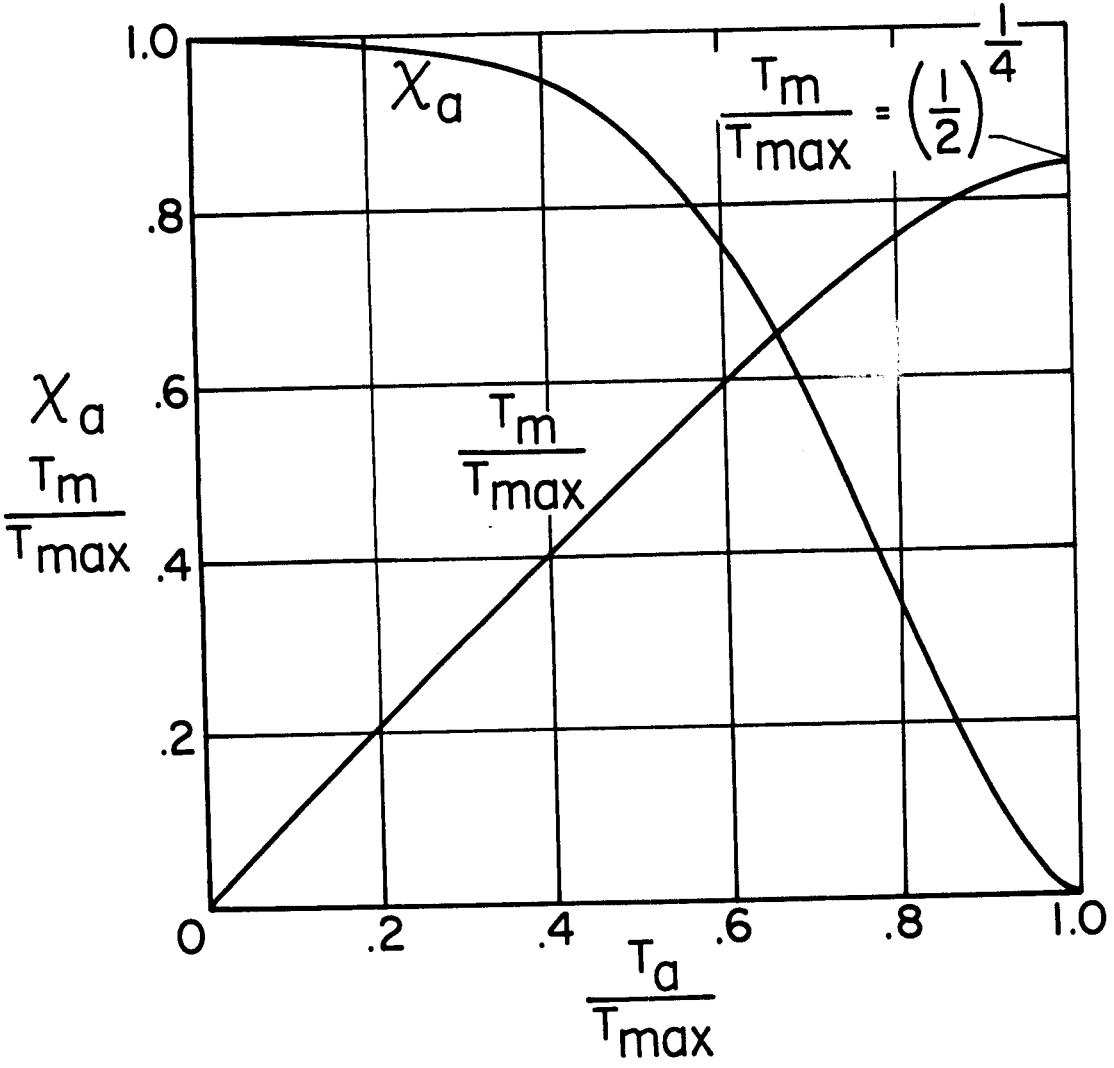

NASA

Figure 5.- Ablation parameters $\frac{T_m}{T_{max}}$ and χ_a.

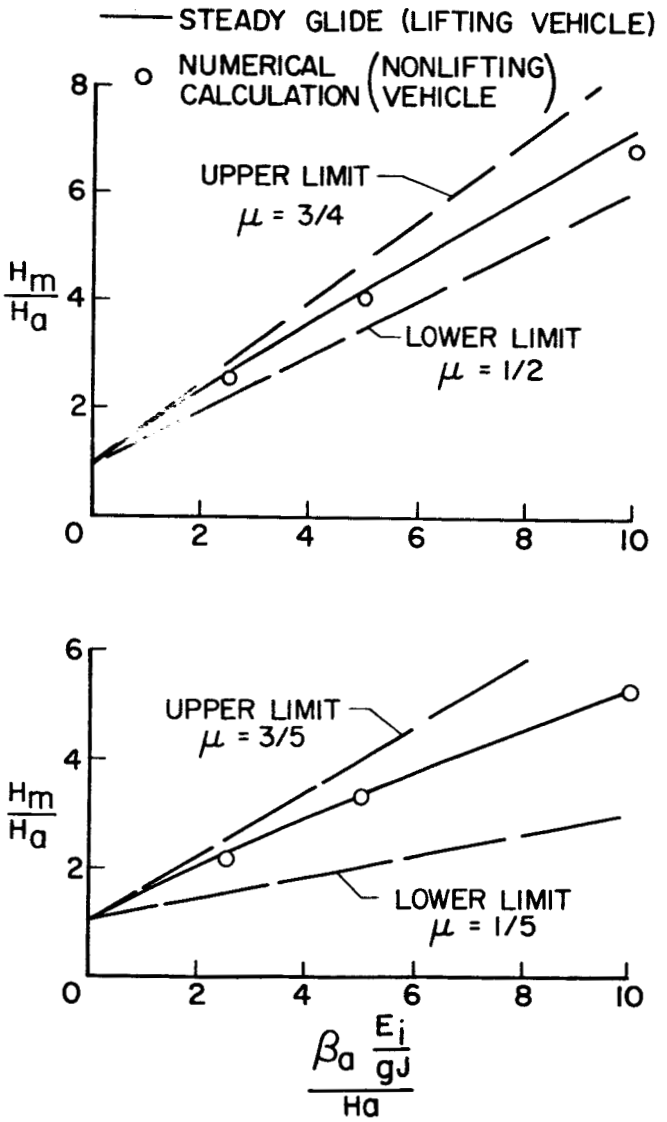

(a) Laminar flow $\left(n = \frac{1}{2}\right)$. (b) Turbulent flow $\left(n = \frac{4}{5}\right)$.

Figure 6.- Dimensionless mean effective heat capacity $\frac{H_m}{H_a}$.

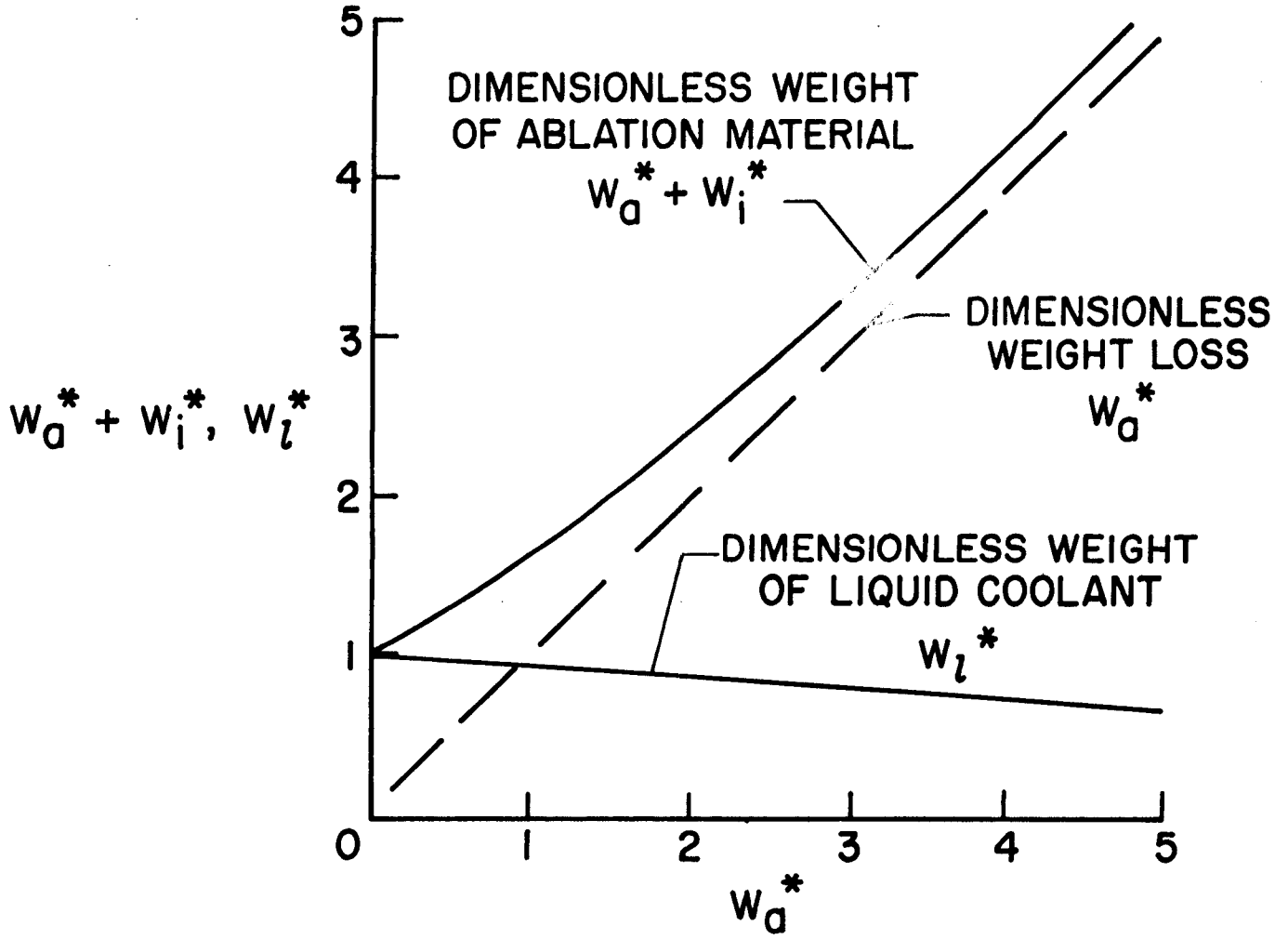

NASA

Figure 7.- Dimensionless weight requirements for a liquid-cooled ablation shield.

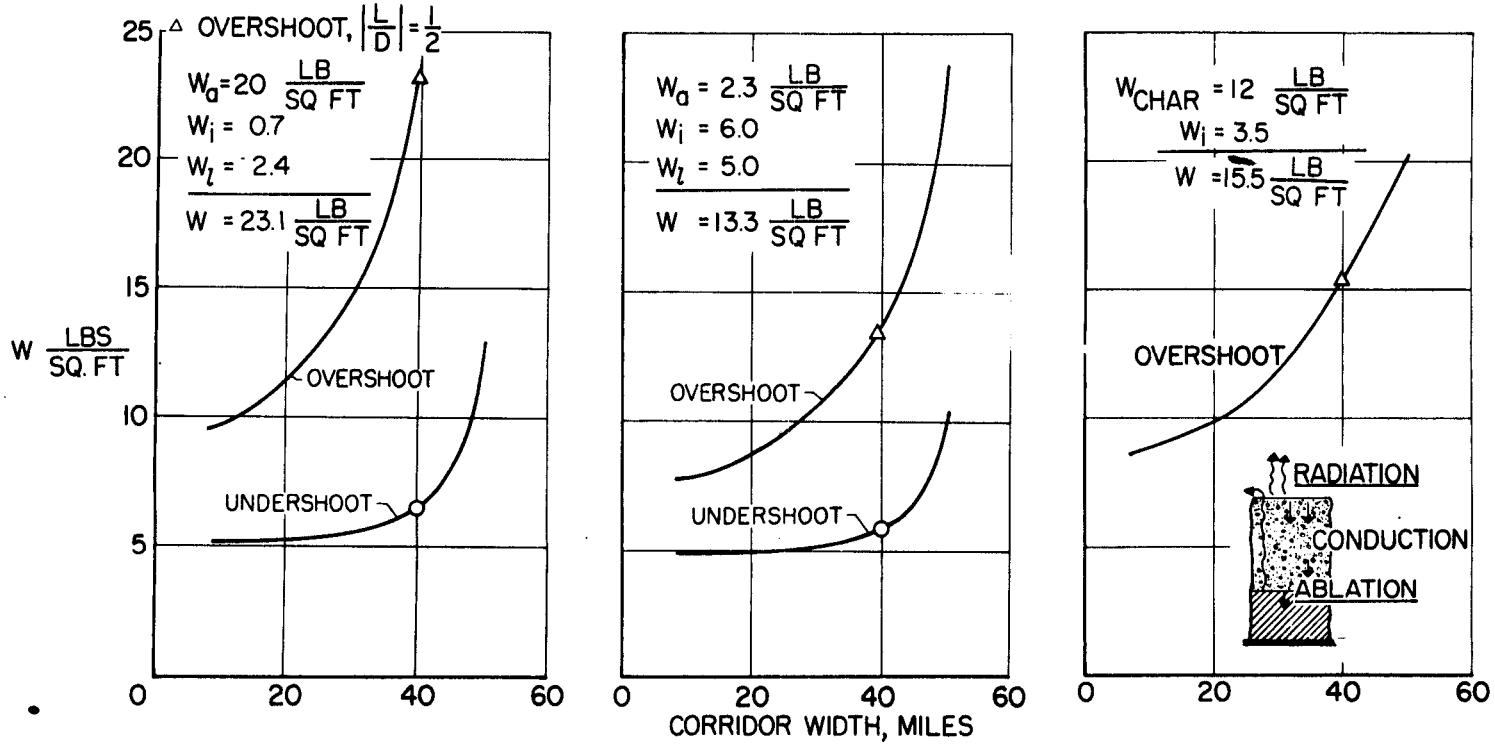

NASA

(a) Low-temperature ablation material (Teflon).

(b) Radiating ablation material (Foamed Quartz).

(c) Composite ablation material (Fiberglas and Phenolic Resin).

Figure 8.- Shield weight per unit area for typical materials $\left[\frac{E_i}{E_c} = 2, \left(\frac{M}{C_{D_{max}} AR} = 1\right) = 1\right]$.

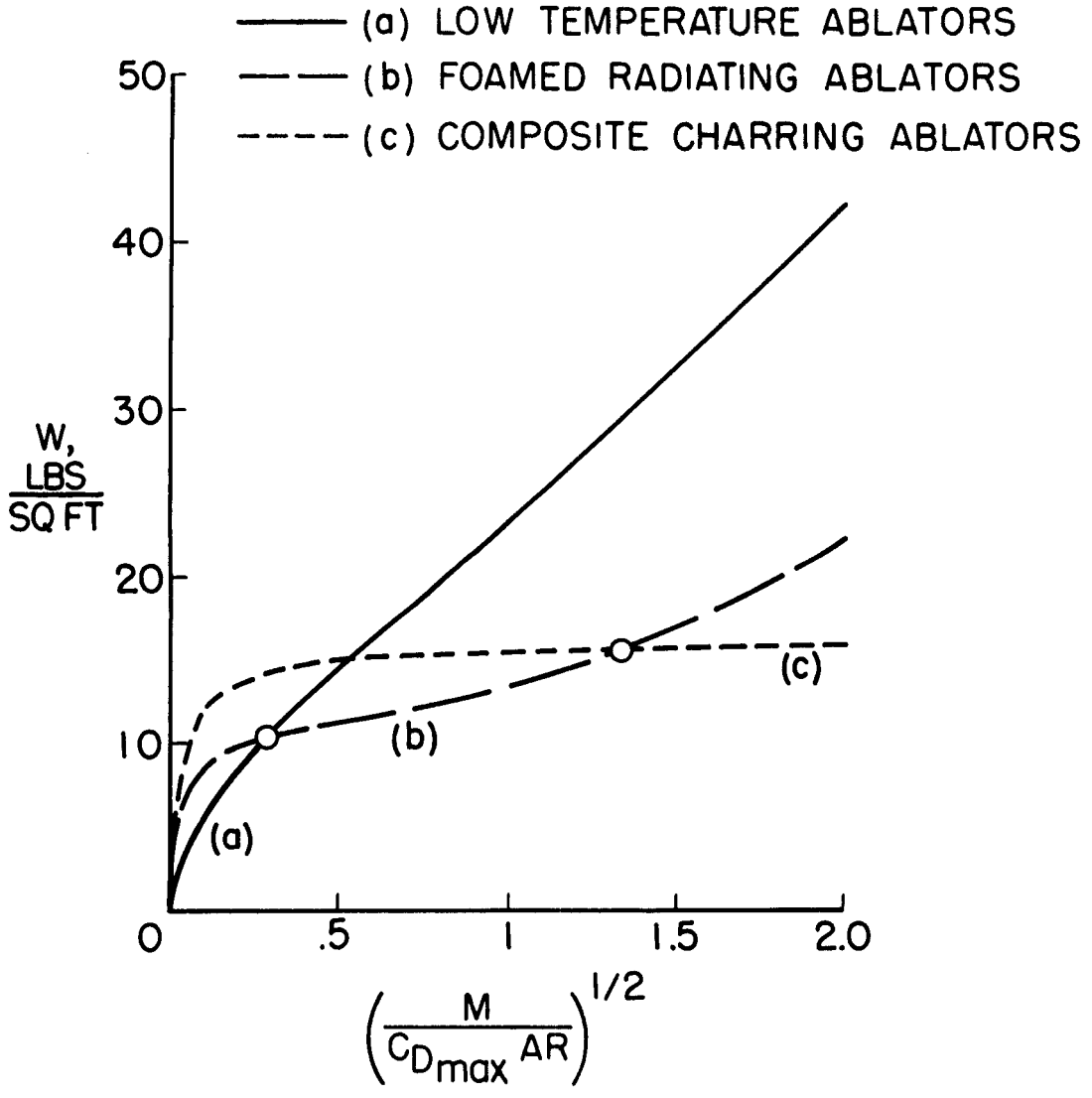

NASA

Figure 9.- Weight comparison of typical materials at overshoot, $\left|\frac{L}{D}\right| = \frac{1}{2}$.

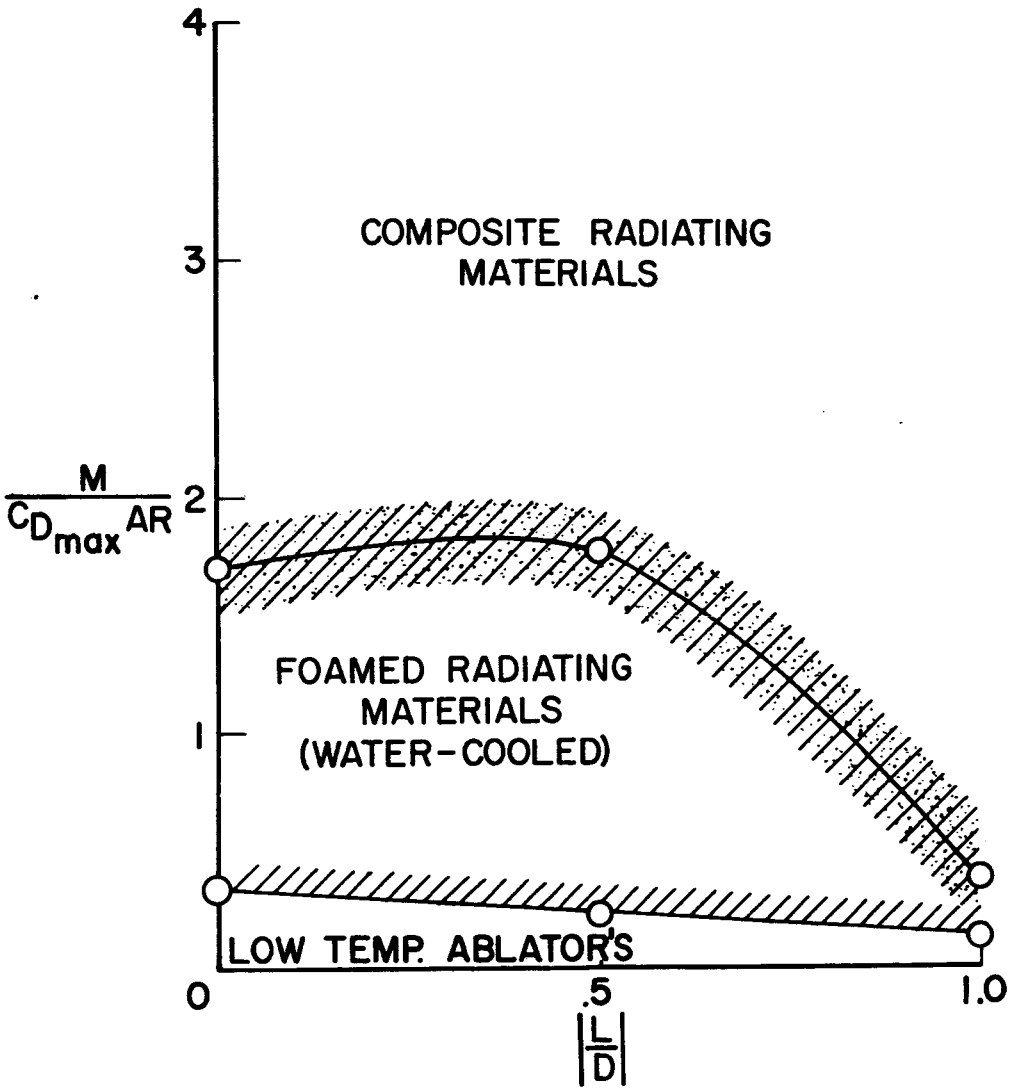

NASA

Figure 10.- Design criteria chart.